

# When mechanical engineering inspired from physiology improves postural-related somatosensory processes

Chloé Sutter<sup>1</sup>, Marie Fabre<sup>1</sup>, Francesco Massi<sup>2,3</sup>, Jean Blouin<sup>1</sup>, Laurence Mouchnino<sup>1\*</sup>

<sup>1</sup> Aix-Marseille Université, CNRS, Laboratoire de Neurosciences Cognitives, FR 3C, Marseille, France, Institut Universitaire de France, Paris

<sup>2</sup> Università degli studi di Roma « La Sapienza »/ Dipartimento di Ingegneria Meccanica ed Aerospaziale

<sup>3</sup> Institut National des Sciences Appliquées de Lyon (INSA LYON), Laboratoire de mécanique des contacts et des structures

\*Corresponding author: Laurence Mouchnino

Aix-Marseille Université, CNRS, Laboratoire de Neurosciences Cognitives, FR 3C  
3 place Victor Hugo, 13331 Marseille, France

Phone : 33 4 13 55 09 47

E-mail : [laurence.mouchnino@univ-amu.fr](mailto:laurence.mouchnino@univ-amu.fr)

37 **ABSTRACT**

38 Being the first stimulated by the relative movement of foot skin and the underneath  
39 moving support surface, the plantar tactile receptors (i.e., mechanoreceptors) play an important  
40 role in the sensorimotor transformation giving rise to a postural reaction. In this light, a  
41 biomimetic surface, i.e., complying with the characteristics of the mechanoreceptors and the  
42 skin dermatoglyphs (i.e., pattern of the ridges) should facilitate the cortical processes in  
43 response to the somatosensory stimulation involved in the balance recovery motor control.  
44 Healthy young adults ( $n = 21$ ) were standing still either on a biomimetic surface or on two  
45 control surfaces (i.e., grooved or smooth), when a sudden but low acceleration of the supporting  
46 surface along the lateral direction was triggered. A shorter and more robust evoked  
47 somatosensory response (i.e., SEP) was observed when participants were standing on the  
48 biomimetic surface. As well, a lower oscillatory response in the theta (5-7 Hz) time-frequency  
49 domain in the left posterior parietal cortex (PPC) was observed with the biomimetic surface.  
50 The greater shear forces induced by the interaction between the feet and the biomimetic surface  
51 during the platform motion was likely at the origin of the increased SEP. Besides, the decrease  
52 of theta power suggests that the balance task became less challenging. This interpretation was  
53 tested in a second experiment by adding a cognitive task, which should be less detrimental for  
54 the postural reaction when standing on a biomimetic surface. Consistent with this hypothesis,  
55 a more efficient postural reaction (i.e., shorter latency and greater amplitude) was observed  
56 when the cognitive task was performed while standing on the biomimetic surface.

57

58

59 **Introduction**

60 During everyday life, unpredictable circumstances can challenge our equilibrium in  
61 different directions while standing. This occurs for example when standing passengers are  
62 subjected to unexpected acceleration and braking manoeuvres in public transport. Exquisitely  
63 compliant, the skin of the foot sole is deformed well before the passenger's reaction to the  
64 driver's manoeuvres. This skin deformation is due to the mechanical interaction (i.e., shear  
65 forces) generated by the surfaces in contact (i.e., the skin of the feet and the supporting surface)  
66 and the gravity force acting on the body mass (i.e., body weight). Although the shear forces are  
67 small relative to the weight force during natural quiet standing, they are readily detectable by  
68 the tactile receptors (Morasso & Schieppati, 1999). These shear forces, and the consequent skin  
69 transient deformations, activate the mechanoreceptors located in the skin allowing the brain to  
70 identify the direction and amplitude of the perturbation, before being detected by other sensory  
71 inputs (e.g. visual, vestibular, or proprioceptive, Mouchnino & Blouin, 2013). These inputs  
72 contribute to shape the postural responses during balance perturbations according to the  
73 identified limits of postural stability (Carpenter et al., 2010; Latash et al., 2003; Mochizuki et  
74 al., 2006; Murnaghan et al., 2011; Riley et al., 1997).

75 The low perceptual threshold for detecting horizontal acceleration of the support surface  
76 (e.g., down to  $0.14 \text{ m/s}^2$  in Mouchnino & Blouin, 2013) suggests a great responsiveness of the  
77 tactile sensory system. This responsiveness could have a twofold origin. First, it could stem  
78 from the richness of the receptor types (fast and slow adaptive, type I or II for the main tactile  
79 receptors) and from the characteristics of the receptors' receptive fields (round to oval in shape,  
80 extended or small, with sharp or blurred boundaries) (Kennedy & Inglis, 2002). It could also  
81 stem from the great compliance (i.e., deformation) of the skin in which the receptors are  
82 embedded, which depends, among others, on the footprint (epidermal ridges) orientation. The  
83 different fingerprint orientations, relative to the textured surface, enhance the subsurface strain  
84 and transmission of tactile information for any direction of the shear forces (Fearing &  
85 Hollerbach, 1985; Prevost et al., 2009). The mechanoreceptors and footprint spatial  
86 characteristics therefore optimise skin deformation, neural encoding of this deformation and  
87 transmission of cutaneous sensory inputs.

88 While the interaction between a surface and the skin has been extensively studied during  
89 finger exploration of a surface (e.g., Hollins & Risner, 2000; Lederman & Klatzky, 2009;  
90 Camillieri et al., 2018; Massimiani et al., 2020; see Basdogan et al., 2020 for a review),  
91 intriguingly, most of the investigations in the field of balance control have ignored the  
92 surface/body contact mechanics. This is particularly surprising given that the foot soles show

93 footprints (dermatoglyphs) that have similar types and density of forms as fingerprints (e.g.,  
94 ~60% of loops are shared by fingerprint and footprints, Sarma, 2020). Skin deformation during  
95 tactile exploration depends not only on the morphological, topographical, and mechanical  
96 properties of the skin, but also from the physio-chemical properties of the surface (i.e.,  
97 materials, topographic features such as height differences, adhesion, spatial period, Cornuault  
98 et al., 2015). In this light, one can hypothesise that the processing of foot cutaneous inputs could  
99 be enhanced when standing on a biomimetic surface, whose texture is inspired by the spatial  
100 characteristics of both mechanoreceptors and dermatoglyphs.

101 Here, to specifically test this hypothesis, we recorded and compared the amplitude of  
102 the cortical evoked somatosensory potential (i.e., P<sub>1</sub>N<sub>1</sub> SEP) when the participants were  
103 standing either on biomimetic or control surfaces, which translated in the lateral direction.  
104 Because it witnesses the amount of sensory input processing at the cortical level (Desmedt &  
105 Robertson, 1977; Hämäläinen et al., 1990; Mauguière et al., 1997; Salinas et al., 2000; Lin et  
106 al., 2003; Case et al., 2016), the amplitude of the P<sub>1</sub>N<sub>1</sub> SEP component was expected to be  
107 greater when the participants stood on a biomimetic surface than on other types of surface (e.g.,  
108 smooth) (*Experiment 1*).

109 Moreover, since an efficient sensory processing allows a better detection of balance  
110 threats, the use of a biomimetic surface should decrease the cognitive demand associated to  
111 equilibrium maintenance during the translation of the support surface. To test this hypothesis,  
112 we compared the changes of sensorimotor theta band power (4-7 Hz) evoked by the translation  
113 of the biomimetic and control surfaces. Indeed, recent studies have shown that an increased  
114 theta power over sensorimotor areas is an electrophysiological biomarker of the increased  
115 difficulty of the balance task. For instance, Sipp et al. (2013) found significant increases of  
116 theta power in the left sensorimotor cortex before imminent rightward or leftward loss of  
117 balance. This localized change of theta power spread afterward over other cortical areas (e.g.,  
118 anterior parietal and anterior cingulate areas). Similar increase of theta band activity was  
119 observed during the preparation of a challenging balance recovery task that required  
120 participants to keep the feet-in place and to refrain stepping responses (Solis-Escalante et al.,  
121 2019). Increased theta band activity is also observed in the PPC during the transition from a  
122 stable to an unstable surface (Hülsdünker et al., 2015; Mierau et al., 2017). This is in line with  
123 de Lafuente & Romo (2006) who showed (in Monkey) responses of the superior PPC to tactile  
124 stimulation which occurred ~60 ms following SI responses. Since the PPC is involved in  
125 sensory information integration and generates decision-related activity (see Romo et

126 de Lafuente 2012 for a review), this associative cortical area is likely involved in motor  
127 recovery response to balance perturbation.

128 Based on the premise that balance control requires a minimum state of attention and of  
129 cognitive resources (Lajoie et al., 1993; Jacobs et al., 2008; Maki & McIlroy, 2007; see  
130 Boisgontier et al., 2011 for a review), facilitating the detection of balance instability when  
131 standing on a biomimetic moving surface should decrease the attentional demand required for  
132 standing steadily. By using a dual task (DT) paradigm (*Experiment 2*) in which participants  
133 were involved in a cognitive task while their supporting surface translated sideways, we  
134 expected smaller interference between the postural and cognitive tasks when participants stood  
135 on a biomimetic surface compared to other surfaces (e.g., smooth). This should result in a better  
136 performance in the cognitive task or a sharper postural reaction to the surface translation (i.e.,  
137 large, short-duration postural reactions, Redfern et al., 2002).

138

## 139 **Methods**

### 140 **EXPERIMENT 1 - Participants and task**

141 Fifteen participants (9 women) without any known neurological and motor disorders  
142 participated in the experiment (mean age  $26 \pm 3$  years, mean weight  $64 \pm 10$ kg). All participants,  
143 except two, characterized themselves as right footed. All participants gave their written  
144 informed consent to take part in this study, which conformed to the ethical standards set out in  
145 the Declaration of Helsinki and which was approved by the CERSTAPS ethic committee.

146 Participants were requested to stand barefoot with their feet at a natural distance apart on  
147 different types of surfaces (see below), fixed in the middle of a movable force platform. They  
148 wore a safety harness attached to the structure top. We ensured that the feet position remained  
149 the same throughout the experimental conditions. As the morphology of foot (i.e., flat, hollow,  
150 standard) can have an impact on body stability (Klein et al., 2008), we verified that none of  
151 them had any foot morphological particularities. This was done by measuring the width of the  
152 forefoot (i.e., metatarsal band from the first to the 5<sup>th</sup> toe) and the isthmus width localized in  
153 the middle of the foot and connecting the forefoot with the rearfoot. Computing the percentage  
154 ratio ((isthmus width)/ (forefoot width)  $\times 100$ ) allowed us to identify hollow feet (<33%),  
155 standard feet (33% to 50%) and flat feet (>50%) (Klein et al., 2008). All participants showed  
156 standard feet, therefore none of them have been excluded from the analyses.

157 We used a set-up employed in previous studies for stimulating foot tactile afferents (e.g.,  
158 Saradjian et al. 2019). A movable force platform is placed on two parallel rails and is held

159 stationary by an electromagnet (Fig. 1A). A cable is attached to the platform and run laterally  
160 through a pulley system with a load fixed to its extremity. The platform translation is triggered  
161 by deactivating the electromagnet. The load is adapted to the weight of the participants, such  
162 that switching off the electromagnet translated the platform very slowly to the right of the  
163 participants, without endangering their balance. A triaxial accelerometer (MEMS, model 4630,  
164 Measurement Specialities, USA; 1000 Hz) was used to measure the platform acceleration  
165 (mean peak acceleration across participants of  $41 \pm 4 \text{ cm.s}^{-2}$ ).

166 At the start of a trial, the participants looked at fixation point positioned at eye level, 2m  
167 directly ahead. They were asked to close their eyes upon receiving the verbal information on  
168 the nature of the upcoming condition, and to remain still. This information indicated one of  
169 these two conditions: platform translation (37 trials) or platform steady (8 trials), which were  
170 pseudo-randomly distributed. The later set of trials reduces the possibility of adopting a  
171 stereotyped postural set linked to the forthcoming body translations. These trials were also used  
172 to measure and model the noise contaminating the EEG data (see below). In all trials, the  
173 participants had to maintain an upright steady posture during 5 s (i.e., duration of trial  
174 recording). The platform translation occurred at any time between 2 s and 4 s after providing  
175 the information about the platform translation to avoid anticipating the instant of the translation  
176 onset. The trials without translation also lasted 5 s. A short break was frequently proposed to  
177 the participants during the experiment.

178

### 179 *Surfaces*

180 Participants were standing on three different surfaces that were glued on the platform: a  
181 biomimetic surface, a textured surface with no bioinspired features characteristics (i.e.,  
182 grooved) and a smooth surface (the last two surfaces were used as controls). These surfaces  
183 were created with a 3D printer (Ultimaker 2+) using biopolymer thermoplastic (Polylactic acid,  
184 PLA). Three characteristics were selected to build the biomimetic surface: shape, spatial period,  
185 and depth of the ridges.

186 The biomimetic surface was textured with circular or oval shapes inspired from both the  
187 shape of the tactile receptors' fields that demonstrate a preferential skin strain axis and  
188 orientation of this axis, which is not the same for all units (Kennedy & Inglis, 2002; Valbo et  
189 al., 1995), and the forms of the dermatoglyphs, which exhibit three main circular forms (loops,  
190 whorls, and arcs, first described by Cummins & Midlo, 1926). We verified whether the radius  
191 of curvature of the circular shape of the biomimetic surface complied with the participants' toe  
192 prints. To do so, we used the ink dabbing method to collect the toe prints of each participant on

193 a white sheet of paper. Contrary to fingerprints, toe prints have their characteristic features in  
194 the lower end of the phalanges (Sarma, 2020). Then, the rolling of the prints was taken  
195 longitudinally from lower end to the upper end of the toe (i.e., opposite direction than when  
196 collecting fingerprints). For each participant, we measured, and then averaged, the radius of  
197 curvature of the 3 most visible ridges from 3 different toes. A t-test of means against a reference  
198 value indicated that the radius of curvature on the toes surface ( $4.3 \pm 1.1$  mm) did not differ  
199 significantly compared to the radius of the loops printed of the biomimetic surface ( $t_{13}= 1$ ,  $p=$   
200 0.34).

201 The spatial period of the biomimetic surface complied with the period of the participants'  
202 toeprints ridges. This was confirmed by the result of the t-test of means against a reference  
203 value showing that the mean period of the biomimetic surface (0.9 mm) was not significantly  
204 different from the period of the toeprints ridges ( $0.87 \pm 0.06$  mm) ( $t_{13}= -1.66$ ,  $p= 0.12$ ). Note  
205 that the spatial period of the biomimetic surface also complied with the distance between the  
206 centre of adjacent receptive fields of the mechanoreceptors (from 0.9 to 3.8 mm; Johansson &  
207 Vallbo, 1983).

208 Finally, the depth of the valley was computed from what we know from finger surface  
209 exploration and balance maintenance literature. The depth to properly perceive the stimulus on  
210 the finger skin is estimated as 0.1 mm with a 0.5 N normal force (Camillieri et al., 2018; Peyre  
211 et al., 2017). In a previous study, we found that the minimum shear forces amplitude to detect  
212 support translation beneath the feet standing in a natural position was  $\sim 3.5$  N (Mouchnino &  
213 Blouin, 2013). This lead to the suggestion that a 0.7 mm depth of the valley should enable to  
214 perceive the minimal shear force when bearing our body weight.

215 A smooth surface also printed in PLA but without any designed patterns was used as a  
216 control surface. While the smooth surface is used as standard control surface, a textured surface  
217 (i.e., grooved surface) with different texture parameters, different from the ones of the  
218 dermatoglyphs and characterized by a main direction, allows for excluding a simple effect of  
219 the local strain variation due to a general texture. Comparing the biomimetic texture with a  
220 standard texture can then highlight the role played by a geometrical distribution of the texture  
221 mimicking the receptive features of the foot skin. Such a biomimetic geometry can give rise to  
222 local stress and strain distributions with a specific orientation pattern, which can favour the  
223 detection of the transient strain variations by the mechanoreceptor activation. The texture of the  
224 grooved surface was composed of rectilinear ridges with a depth of 0.3 mm and a period of 7  
225 mm.

226 The order of the 3 surface expositions was counterbalanced across participants. The  
227 participants were not informed prior to the experiment about the reason the standing surface  
228 was changed during the recording session. When the participants were asked after the  
229 experiment whether they had perceived that they stood on surfaces having different textures,  
230 none of them reported having done so.

231

232 *Recordings and analyses*

233 Electroencephalography (EEG) activity was continuously recorded from 64 Ag/AgCl  
234 surface electrodes embedded in an elastic cap (BioSemi ActiveTwo system: BioSemi,  
235 Netherlands). Specific to the BioSemi system, “ground” electrodes were replaced by Common  
236 Mode Sense active and Driven Right Leg passive electrodes. The signals were pre-amplified at  
237 the electrode sites, post amplified with DC amplifiers, and digitized at a sampling rate of 1024  
238 Hz (Actiview acquisition program). The signals of each electrode were referenced to the mean  
239 signal of all electrodes. Four Ag/AgCl electrodes placed near the canthus of each eye and  
240 under/over the left eye orbital allowed us to control for blinks, and horizontal and vertical eye  
241 movements.

242 The continuous EEG signal was segmented into epochs synchronized relative to the onset  
243 of the platform translation, which was identified at the onset of the monotonic increase of the  
244 shear force. After artefact rejections based on visual inspection, for each participant and surface,  
245 a minimum of 96% of the trials were included in the analyses. The signals were filtered off-line  
246 with a 50 Hz digital notch filter (24 dB/octave) and with a 0.1–48 Hz band-pass digital filter  
247 (48 dB/octave) implemented in BrainVision Analyzer 2 software (Brain Products, Germany).  
248 For each participant, the SEPs were obtained by averaging all epochs of each surface for each  
249 participant. The average amplitude computed 50 ms prior to the platform translation served as  
250 baseline. Consistent with studies recording cortical potentials evoked by lower limb stimulation  
251 (Altenmüller et al., 1995, Saradjian et al., 2013), the SEPs were found to be maximal over the  
252 vertex (Cz electrode). Therefore, this electrode was used to assess the SEPs. We primarily based  
253 our analyses on the P<sub>1</sub>N<sub>1</sub> wave evoked by the sensory stimulation induced by the platform  
254 translation. The amplitude of P<sub>1</sub>N<sub>1</sub> was measured peak to peak, and its latency was assessed  
255 measuring the P<sub>1</sub> latency.

256

257 *Cortical sources*

258 Neural sources of the SEPs were estimated with the dynamical Statistical Parametric  
259 Mapping (dSPM, Dale et al., 2000) implemented in the Brainstorm software. A boundary  
260 element model (BEM) with three realistic layers (scalp, inner skull, and outer skull) was used  
261 to compute the forward model on the anatomical MRI brain template from the Montreal  
262 Neurological Institute (MNI Colin27). Using a realistic model has been shown to provide more  
263 accurate solution than a simple three concentric spheres model (Sohrabpour et al, 2015). We  
264 used of a high number of vertices (i.e., 15 002 vertices) to enhance the spatial resolution of the  
265 brain template. Such EEG source reconstruction has proved to be suited for investigating the  
266 activity of outer and inner cortical surfaces with 64 sensors (Chand & Dhamala, 2017; Ponz et  
267 al., 2014). Measuring and modelling the noise contaminating the EEG data is beneficial to  
268 source estimation. Noise covariance matrices were computed using the 8 trials with the platform  
269 steady condition, while the participants stood still. The current maps were averaged from the  
270 start of the shear forces to N1, for each participant and surface condition.

271 The data were transformed into time-frequency domain using Morlet wavelet transforms.  
272 We used a 1 Hz central frequency (full width at half maximum FWHM tc=3sec) which offers  
273 a good compromise between temporal and spectral resolutions (Allen & MacKinnon, 2010).  
274 The power of theta (5-7 Hz) was computed for each trial in the source space in a region of  
275 interest (ROI, 589 vertices) encompassing the left inferior and superior PPC (based on the  
276 Destrieux cortical atlas, Destrieux et al., 2010). Then, the signal was expressed as a change of  
277 theta power computed over the first 400 ms of the platform translation (which included the  
278 P1N1 SEP) with respect to a 350 ms window baseline taken before the translation (-400 to -50  
279 ms). For each participant, the resulting event-related synchronization/desynchronization  
280 (ERS/ERD) was then averaged across trials and surface conditions. The same procedure was  
281 applied with the signals computed in a control ROI (650 vertices) encompassing the inferior  
282 and superior PPC of the right hemisphere.

283 *Behavioural recordings and analyses*

284 The ground reaction forces and moments were recorded with an AMTI force platform (60  
285 × 120 cm, Advanced Mechanical Technology Inc., USA) at a sampling rate of 1000 Hz. The  
286 ground reaction shear forces were analysed along the mediolateral (M/L) axis, as they represent  
287 the earliest signature of the cutaneous stimulation evoked by the platform translation. The onset  
288 of this stimulation was defined as the first time the M/L shear force started to increase  
289 monotonically. Figure 1B shows and the dynamics of the M/L shear forces resulting from the  
290 platform acceleration.

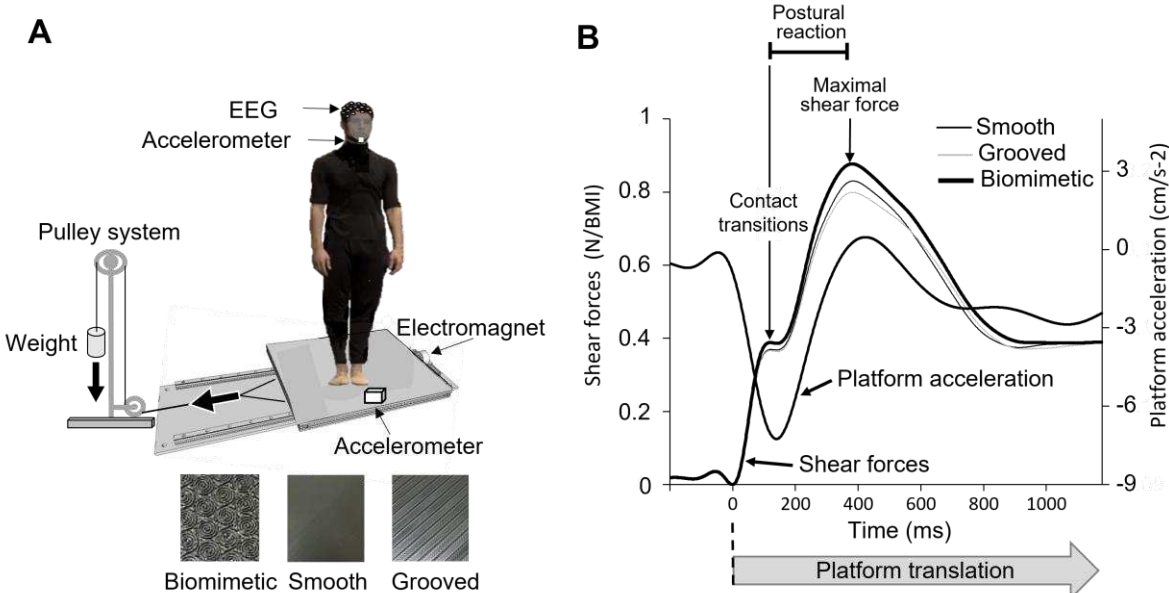
291 A general pattern of events emerged:

292 i) the first phase shows a ramp of the platform acceleration (constant jerk) corresponding to a  
293 ramp in the traction force; this phase lasted on average  $197 \pm 11$ ms leading to a platform  
294 displacement of about  $2.93 \pm 0.30$  mm. Due to the inertia of the body, this displacement is  
295 accommodated mainly by the skin deformation. The peak amplitude of this force was measured  
296 with respect to its baseline value (i.e., prior to the translation onset);

297 ii) in a following transition phase, a low valley was observed; the jerk decreases and becomes  
298 negative. This is a crucial phase, where the contact between the skin and the surface is  
299 characterized by high superficial shearing, leading to transient variations of the local strain  
300 distribution (“*skin-surface contact transitions*”), which are directly affected by the topography  
301 of both the skin and the surface itself; moreover, local detachments and slipping can occur,  
302 leading to transient deformations and waves propagating in the skin, which are likely to activate  
303 the mechanoreceptors (“*contact stimuli*”); a similar phenomenon has been observed in  
304 literature, when considering the motion of a surface under a stationary fingertip, showing that  
305 the deformation of the skin increases until the frictional force (i.e., shear force) cannot anymore  
306 resist the sliding (i.e., stick/slip phenomenon, Rabinowicz 1956); within this phase, the shear  
307 forces result from a balance between inertia effects and contact accommodation.

308 iii) Afterwards the shear forces continued to increase in the same direction until a second peak  
309 was reached before reversing the forces. This second increase can be considered as a postural  
310 reaction (Lhomond et al., 2021; Saradjian et al., 2019). The duration of the postural reaction  
311 was defined as the time elapsed between these peaks.

312 The amplitudes of both peaks of the shear forces were normalized to the body mass index (BMI)  
313 of each participant.



314

315

316 **Figure 1. A. Experimental set up.** The participant stood on one of the three surfaces glued on  
317 the force platform which, on deactivation of the electromagnet, would undergo a translation to  
318 gravity loading. They wore a safety harness (not shown in the figure) attached to the structure  
319 top. **B. Mean lateral forces and platform acceleration of the 15 participants.** At the platform  
320 translation onset (broken line) two consecutive phases in lateral force were observed. The first  
321 peak force corresponds to the maximal extensibility of the skin under the feet until the frictional  
322 force (i.e., shear force) cannot anymore resist the sliding leading to transient variations of the  
323 local strain distribution (“skin-surface contact transitions”). Afterwards, a second force peak  
324 occurred and corresponds to a postural reaction.

325

326 Head acceleration was measured with a triaxial accelerometer (model 4630, Measurement  
327 Specialities, USA; 1000 Hz) placed on the participants’ chin. We measured head acceleration  
328 to evaluate the latency of the vestibular stimulation induced by the platform translation. The  
329 onset of the vestibular stimulation was defined at the first moment head acceleration exceeded  
330 0.048 m.s<sup>-2</sup> (i.e., threshold for vestibular stimulation, Gianna et al. 1996). We measured the lag  
331 between the head acceleration and the shear forces to determine if the vestibular stimulation  
332 occurred after the stimulation of the foot mechanoreceptors.

333 Bipolar surface electromyography (EMG, Bortec AMT-8 system, Bortec Biomedical,  
334 Canada) was used to record the activity of the long fibular muscle (FL) of both legs. The FL  
335 muscles are responsible (with other muscles) for controlling stance. They contribute to the  
336 eversion movement of the foot, and also to the maintenance of the arch of the foot to ensure  
337 optimal postural stability (Pietrosimone & Gribble, 2012; Jeon et al., 2021). The FL EMG  
338 signals were pre-amplified at the skin site ( $\times 1000$ ), sampled at 1000 Hz, band pass filtered from  
339 20 to 250 Hz, and rectified. Two participants were excluded from the EMG analyses due to

340 noisy EMG signals. To quantify the muscle activity, we computed the integral of the EMG  
341 activity (iEMG) over two intervals. The first corresponded to the “resting interval”. It lasted 1s  
342 and ended at the onset of the platform translation. The second interval covered the time elapsed  
343 between the platform onset and the N1 component of the SEP. The duration of this second  
344 period was specific to each participant. In order to be able to compare muscle activities between  
345 the two intervals, we normalized, for each participant, the EMG activity of the resting interval  
346 to the duration of the second interval “N1 latency” (~180ms). We also calculated the latencies  
347 of EMG changes relative to the onset of the platform translation. This was done by first  
348 computing the mean and standard deviation of the muscle background activity (i.e., during the  
349 resting interval) for each participant and surface. The onsets of the EMG increased, or decreased  
350 activities were defined as the times at which the EMG activity increased above or decreased  
351 below a threshold level set at twice the standard deviation of the mean background activity.

352

### 353 **EXPERIMENT 2 - Participants and task**

354 The goal of *Experiment 2* was to test whether the attentional demand required for  
355 equilibrium maintenance is reduced when standing on the biomimetic surface, compared to a  
356 control surface. To further compare the effect between standing on a biomimetic and standing  
357 on a non-biomimetic textured surfaces, the grooved surface used in *Experiment 1* was selected  
358 as the control surface.

359 Twenty-one new participants (7 women) without any known neurological and motor  
360 disorders participated in the experiment (mean age  $22 \pm 2$  years, mean weight  $67 \pm 10$ kg). All  
361 participants gave their written informed consent to take part in this study, which conformed to  
362 the ethical standards set out in the Declaration of Helsinki and which was approved by the  
363 CERSTAPS ethic committee.

364 The procedure was identical to that in *Experiment 1* with one exception that pertained to  
365 the dual task (DT) paradigm. We used a demanding cognitive task to increase the participants’  
366 attentional load while their supporting surface was translated as in *Experiment 1*. Participants  
367 were asked to listen to a series of 10 different three-digit numbers (1Hz) that ended 60ms before  
368 the platform translation. The 10 numbers were spelled out at high speed (being completed in  
369 10 s) by a computer voice. The series of numbers varied across trials but were the same for both  
370 surface conditions and participants. Participants were instructed to count silently the number of  
371 times that 7 was part of the three-digit numbers and to provide their response at an auditory  
372 tone occurring 3 s after the platform translation onset (i.e., after the data analysed intervals).  
373 The same procedure was used for the trials in the steady platform condition. We

374 counterbalanced the presentation of the different conditions (i.e., biomimetic or grooved  
375 surfaces, with or without translation; single or dual tasks) across participants but prevented the  
376 occurrence of 2 successive conditions involving the dual task.

377 The participants' performance in the cognitive task was assessed by computing, for each  
378 surface condition, the averaged percentage of errors ((number of errors/10 numbers) x 100). An  
379 error was counted each time that the participant reported a wrong number of times that 7 was  
380 part of the spelled-out numbers.

381

### 382 *Statistical analyses*

383 The behavioural and EEG data were submitted to separate analysis of variance  
384 (ANOVA) with repeated measurements. In *Experiment 1*, one-way ANOVAs were used for  
385 mean comparisons with the support surface (Smooth, Grooved, Biomimetic) as intra-  
386 participants factor. We computed statistical maps by contrasting the current maps (i.e., each  
387 vertice) computed when standing on a biomimetic surface and control surfaces using t-tests  
388 (significance threshold  $p < 0.05$ ) (Tadel et al., 2011). We applied an FDR (False Discovery  
389 Rate) correction for multiple comparisons across regions (Benjamini & Hochberg, 1995).  
390 In *Experiment 2*, a 2x2 ANOVA was used for mean comparisons with the support surface  
391 (Grooved, Biomimetic) and task (single or dual task) as intra-participants factors. Significant  
392 effects (statistical threshold of  $p \leq 0.05$ ) were further analysed using Newman-Keuls post-hoc  
393 tests.

394

## 395 **Experiment 1**

### 396 **Results**

#### 397 *Augmented peripheral stimulation by the biomimetic design of the surface*

398 As shown in Fig. 1B, the shear forces increased in the leftward direction at the onset of  
399 the rightward platform translation until a clear break down point was reached (see methods).  
400 The results showed that the amplitude of this early force differed significantly between surfaces  
401 (Fig. 2B;  $F_{2,28} = 13.84$ ,  $p < 0.05$ ). Post-hoc analyses revealed that the amplitude was greater for  
402 the biomimetic ( $0.40 \pm 0.05$  N/BMI) than for the grooved and smooth surfaces ( $Ps < 0.05$ ),  
403 which did not differ significantly ( $p = 0.20$ ; overall mean of  $0.38 \pm 0.05$  N/BMI).  
404 The latency of the break down point did not depend on the surface (overall mean of  $117 \pm 12$ ms;  
405  $F_{2,28} = 0.12$ ,  $p = 0.89$ ). It occurred before reaching the maximal value of the platform acceleration  
406 (overall mean  $-26 \pm 11$ ms) for all surfaces (no significant surface effect  $F_{2,28} = 2.09$ ,  $p = 0.14$ );

407 this suggested that the early peak of the shear forces was not generated by the reaching of the  
 408 maximum acceleration of the platform and the consequent change in the sign of the jerk.  
 409 In addition, the EMG analyses (Fig. 2A) showed that the activity of the right FL muscle started  
 410 to increase  $40 \pm 20$  ms after the break down point and that the latencies of these increases were  
 411 not significantly affected by the surface ( $F_{2,24} = 0.64$ ;  $p = 0.54$ ). The left FL activity decreased  
 412 simultaneously with the right FL activation in 10 out to 13 participants. The delay of the  
 413 changes in the FL muscles activities relative to the break down point suggested that the early  
 414 shear forces were not muscularly induced, but rather passively/mechanically evoked by the  
 415 contact transmission between the stretched skin and the platform.  
 416 Besides, the observations that only the right FL (among the 2 recorded muscles) started to be  
 417 activated after the “skin-surface contact transitions” (i.e., during the postural reaction, Fig. 2A)  
 418 suggested that it was engaged in the breaking of balance perturbation. The postural reaction  
 419 was not altered by the surface conditions, neither for its amplitude ( $F_{2,28} = 2.50$ ;  $p = 0.10$ , mean  
 420  $= 0.53 \pm 0.10$  N/BMI) nor for its duration ( $F_{2,28} = 0.20$ ;  $p = 0.82$ , mean  $= 296 \pm 64$  ms). The head  
 421 started moving (i.e., accelerate) during the postural reaction with a latency of  $172 \pm 38$  ms  
 422 relative to the platform translation (Fig. 2A). This lag, which likely resulted from the body mass  
 423 inertia, was not significantly affected by the surface condition ( $F_{2,28} = 1.48$ ;  $p = 0.25$ ).  
 424

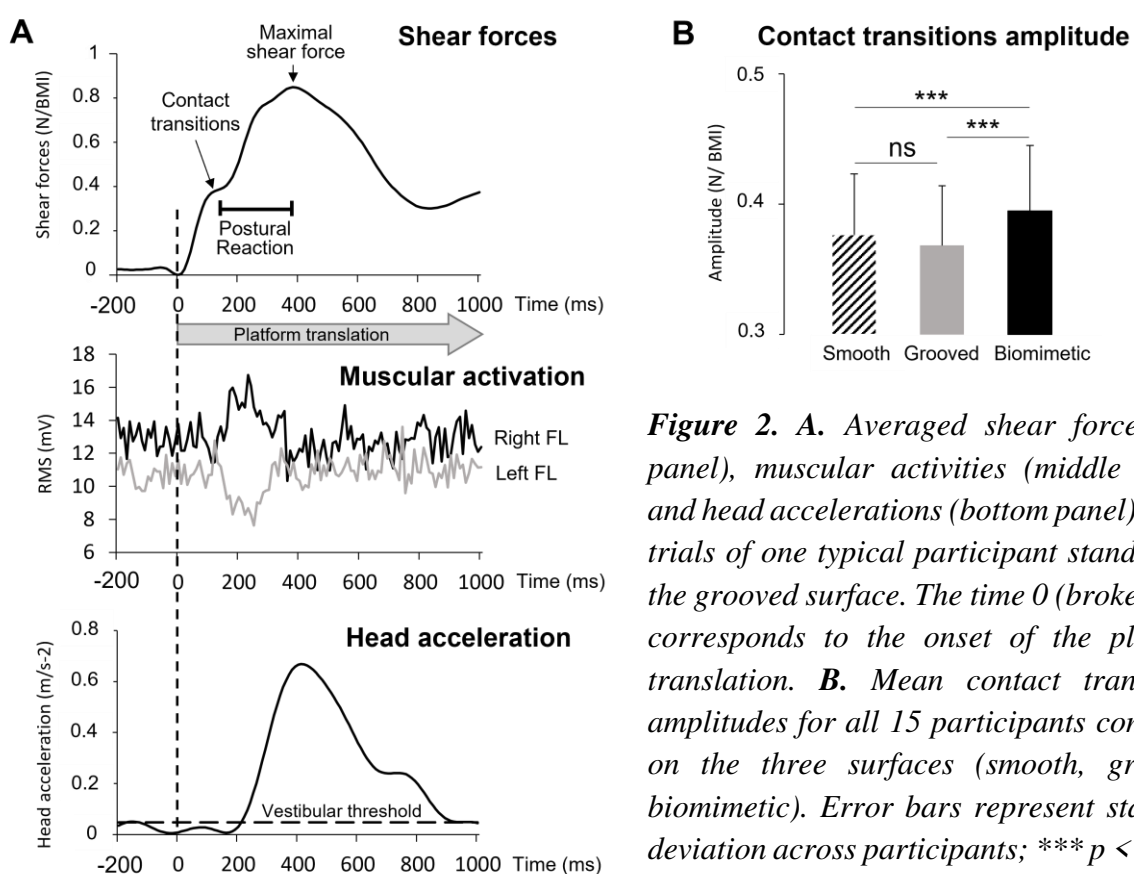


**Figure 2.** **A.** Averaged shear forces (top panel), muscular activities (middle panel) and head accelerations (bottom panel) for all trials of one typical participant standing on the grooved surface. The time 0 (broken line) corresponds to the onset of the platform translation. **B.** Mean contact transitions amplitudes for all 15 participants computed on the three surfaces (smooth, grooved, biomimetic). Error bars represent standard deviation across participants; \*\*\* $p < 0.001$ , ns = not significant.

426 *Cortical facilitation of sensory input when standing on a biomimetic surface*

427 To determine whether the SEP (i.e., P<sub>1</sub>N<sub>1</sub>) originated from tactile and/or vestibular  
428 peripheral inputs, we compared the latencies of P<sub>1</sub> and N<sub>1</sub> to the vestibular stimulation onset.  
429 The onset of the vestibular stimulation was defined at the first moment head acceleration  
430 exceeded 0.048 m.s<sup>-2</sup> (i.e., threshold for vestibular stimulation, Gianna et al. 1996). This  
431 threshold latency was not significantly affected by the surface condition (F<sub>2,28</sub>= 1.75; p =  
432 0.19). Paired t-tests showed that P<sub>1</sub> and N<sub>1</sub> latencies significantly preceded vestibular  
433 stimulation onset for all the surfaces (see Table 1). This indicated that the SEP was not evoked  
434 by vestibular inputs, but more likely by cutaneous inputs originated from the shear forces (i.e.,  
435 skin strain) evoked by the platform translation.

436

<i>Smooth</i>		<i>Grooved</i>		<i>Biomimetic</i>	
<b>Vestibular threshold</b>					
211ms (±40)		225ms (±27)		207ms (±32)	
<b>P1</b>	<b>N1</b>	<b>P1</b>	<b>N1</b>	<b>P1</b>	<b>N1</b>
138ms (±11)	186ms (±15)	137ms (±13)	184ms (±18)	126ms (±16)	187ms (±13)
<b>T test</b>					
t = 7.09 ; p<0.001	t = 2.79 ; p = 0.01	t = 12.12; p<0.001	t = 5.50; p<0.001	t = 9.93; p<0.001	t = 2.68 ; p = 0.02

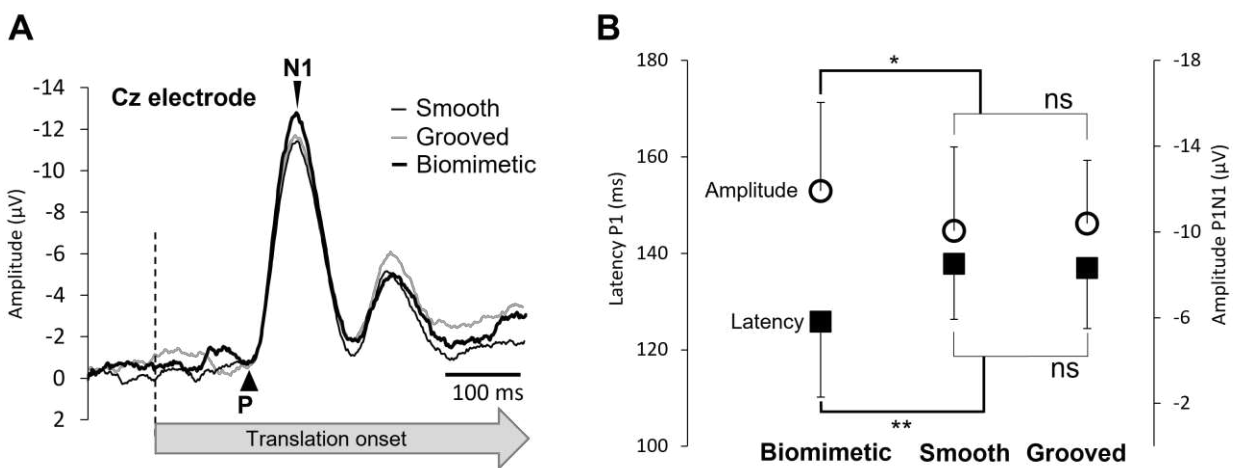
437

438

439 **Table 1.** Mean latencies of all participants (n = 15) and inter participants standard deviation  
440 (SD) for the P<sub>1</sub>, N<sub>1</sub> and the time when the head reached the vestibular threshold as a function  
441 of the surfaces on which participants were standing. The paired t test corresponds to the  
442 comparison between the P<sub>1</sub> or N<sub>1</sub> and the vestibular threshold.

443

444 Importantly, the latency of P<sub>1</sub> was shorter and the amplitude of the P<sub>1</sub>N<sub>1</sub> was greater for  
445 the biomimetic surface than for the smooth and grooved surfaces (Fig. 3). The significant main  
446 effect of the surface condition (contact stress and strain distribution obtained by the biomimetic  
447 topography) was confirmed by the P<sub>1</sub> latency (F<sub>2,28</sub> = 6.65, p = 0.004) and the P<sub>1</sub>N<sub>1</sub> amplitude  
448 (F<sub>2,28</sub> = 3.55, p = 0.04), which did not show difference between the two control surfaces either  
449 for P<sub>1</sub> latency (p= 0.81) or P<sub>1</sub>N<sub>1</sub> amplitude (p= 0.65). There was no significant effect of surface  
450 on N<sub>1</sub> latency (F<sub>2,28</sub>= 0.41, p= 0.67).



451

452 **Figure 3. A.** Grand average ( $n=15$ ) of the SEP recorded over Cz electrode for the 3 surfaces  
453 (biomimetic, smooth, grooved). The broken line indicates the moment of the stimulation (i.e.,  
454 translation onset). **B.** Mean P1 latency and amplitude of the averaged P1N1 SEP for all  
455 participants on the three surfaces (biomimetic, smooth, grooved). Error bars represent  
456 standard deviation across participants, \* $p < 0.05$ ; \*\* $p < 0.01$ ; ns = not significant.

457

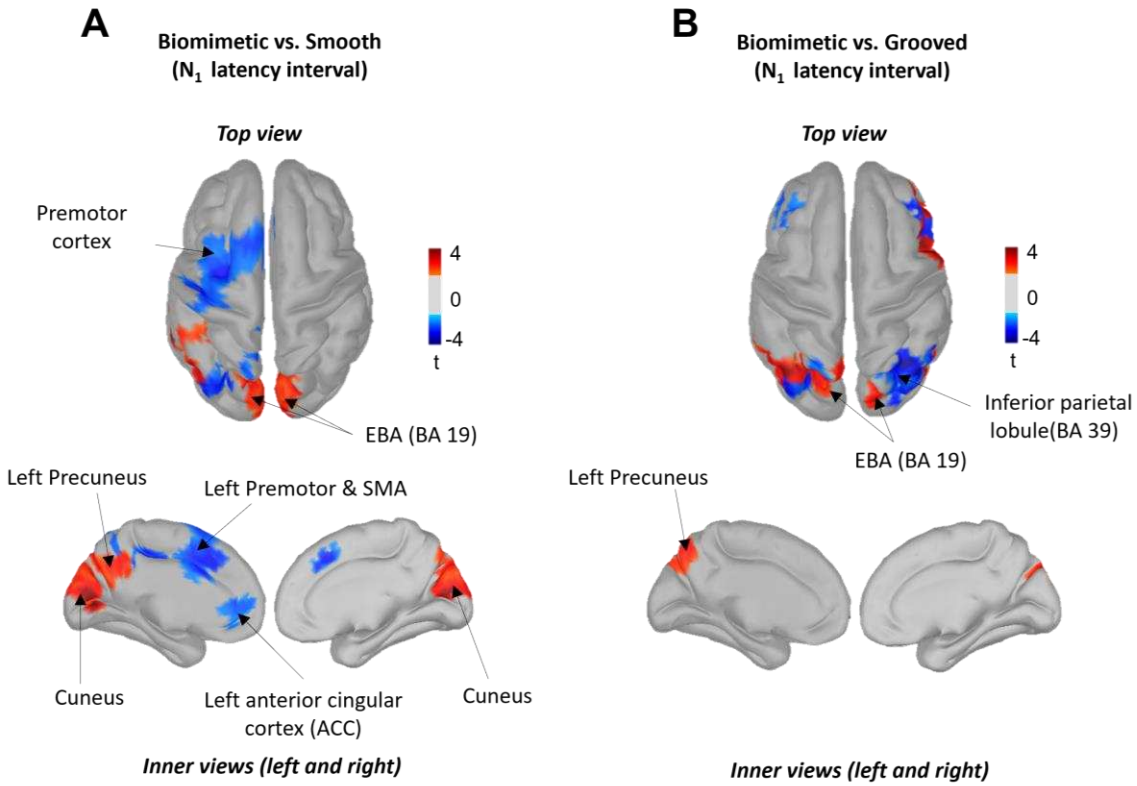
458 To verify if the SEP facilitation (i.e., shorter P<sub>1</sub> latency and greater P<sub>1</sub>N<sub>1</sub> amplitude) observed with the biomimetic surface could be linked to a change in leg muscle activity, we  
459 compared the iEMG of the right and left FL during the N<sub>1</sub> latency interval. The ANOVA did  
460 not show a surface condition effect on the iEMG ( $F_{2,24} = 0.57$ ;  $p = 0.57$  and  $F_{2,24} = 1.11$ ;  $p = 0.34$ ,  
461 for the right and left FL, respectively). These results suggest that the changes in the SEP  
462 observed over the somatosensory cortex when the participants stood on the biomimetic surface  
463 stemmed from an increased afferent volley from the foot sole mechanoreceptors rather than  
464 from an altered motor command (i.e., muscle activity).

466

#### 467 Standing surface-specific source localization

468 The statistical cortical maps revealed significant greater activation (i.e., current) in the  
469 left precuneus (medial extent of Brodmann area 7, warm colour) for the biomimetic surface for  
470 both the biomimetic/smooth (Fig. 4A) and biomimetic/grooved (Fig. 4B) contrasts. The same  
471 contrasts also showed significantly greater activity of the extrastriate body areas (EBA, BA19).  
472 On the other hand, these contrasts revealed greater activities of the left premotor (PM) and  
473 anterior cingulate (ACC) cortices (see cold colors in Fig. 4A) for the smooth surface and greater  
474 activation of the right inferior PPC (BA39) for the grooved surface (Fig. 4B, cold colour).

475



476

477

478 **Figure 4.** Statistical source estimation maps for Biomimetic versus Smooth (A), Biomimetic  
479 versus Grooved (B) contrasts. Significant t-values ( $p \leq 0.05$ ,  $n = 15$ ) of the source localization  
480 were shown during the time window from 0 ms to N1 latency. Sources are projected on a  
481 cortical template (MNI's Colin 27). For each contrast, we display the top and the left and right  
482 inner cortical views.

483

484 Modulation of theta (5-7 Hz) oscillations in the left PPC

485 The time-frequency analysis showed that theta power computed in the left PPC was  
486 significantly modulated by the type of surface on which the participants were standing ( $F_{2,28} =$   
487 3.99;  $p = 0.03$ ). Post-hoc analyses revealed that theta power was significantly smaller for the  
488 biomimetic than for the smooth and grooved surfaces ( $p < 0.05$ ), with no significant difference  
489 between the two control surfaces ( $p = 0.67$ ,  $ps > 0.05$ ) (Fig. 5C). This effect was lateralized to  
490 the left hemisphere as it was not observed in the right PPC ( $F_{2,28} = 1.32$ ;  $p = 0.28$ ).

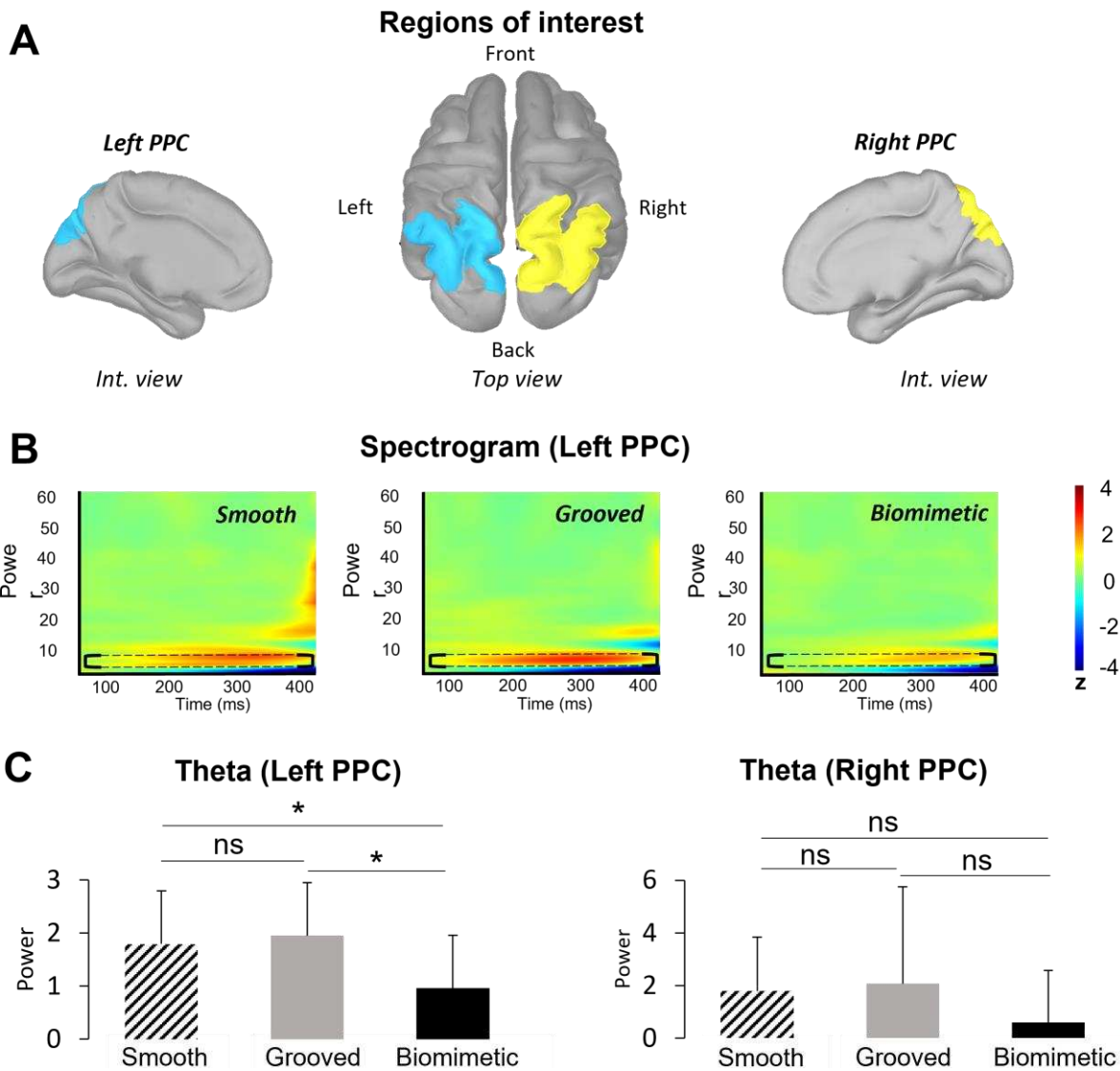


**Figure 5. A.** Localization of the regions of interest (ROIs) on the anatomical MRI Colin 27 brain template that was used to compute cortical activations. Note that similar ROIs were defined for the left and right Parietal Posterior Cortex (PPC). **B.** Time-frequency power (ERS/ERD) of the signals by means of a complex Morlet's wavelet transform applied on the ROIs for each surface of each participant then averaged. Cooler colors indicate ERD and warmer colors, indicates ERS. Frequency bands from 1 to 90 Hz were provided to have an overview of the full spectral content of cortical neural oscillations. We showed the spectrum from 0 to 400 ms to focus on the analyzed time window of the ERS/ERD (thereby removing edge effects). The theta band has been circled in dotted line for each surface. **C.** Mean of theta (5-7 Hz) frequency band computed during (0; 400 ms) time window in the left and right PPC for each surfaces (smooth, grooved, biomimetic). Error bars are standard error across participants, \*  $p < 0.05$ , ns = not significant

506 **Discussion**

507 *Standing on a biomimetic surface speeds up and enhances the sensory transmission from foot*  
508 *to cortical areas*

509 Complying with both dermatoglyphs and mechanoreceptors characteristics, the  
510 biomimetic surface in interaction with the feet evoked faster and greater cortical response to  
511 the platform translation (i.e., P<sub>1</sub>N<sub>1</sub>), with respect to both control surfaces (i.e., grooved and  
512 smooth). The greater amplitude of the SEP, when standing on the biomimetic surface, suggests  
513 augmented cutaneous afferent processes (see Desmedt & Robertson, 1977; Hääläinen et al.,  
514 1990; Salinas et al., 2000; Lin et al., 2003; Case et al., 2016; Lhomond et al., 2016). The  
515 increase P<sub>1</sub>N<sub>1</sub> amplitude and the shortening of the evoked response latency (i.e., P<sub>1</sub>) could be  
516 due to an accentuation of the deformation of the skin when interacting with the biomimetic  
517 surface. The enhanced skin transient deformations was witnessed by an increase amplitude of  
518 the peak force during the “skin-surface contact transitions” while no concomitant change of its  
519 duration was observed. This is in line with Tang et al.’s (2020) study showing that a greater  
520 deformation of the fingers’ skin generates greater friction force, and stress that induce stronger  
521 tactile stimulation of the mechanoreceptors. Similarly, the interaction of the foot and the  
522 biomimetic surface increased the intensity of the skin mechanoreceptors stimulation, which in  
523 turn boosted the transmission of cutaneous signals to the primary somatosensory cortex (SI)  
524 where neurons respond to various tactile stimulations (e.g., Bensmaia et al., 2008; Weber et al.,  
525 2013).

526 Our source analyses showed that changing the standing surface significantly altered the  
527 current recorded in the left PPC but had no significant effect on the current recorded in SI. This  
528 suggests that the sensory facilitation observed with the biomimetic surface may have involved  
529 direct thalamocortical projections to the PPC. The basis for this suggestion is twofold. First,  
530 neuroanatomical studies in the macaque have shown direct projections of cutaneous  
531 information from the thalamus to the PPC (Pearson et al., 1978; Padberg et al., 2009; Impieri  
532 et al., 2018; Gamberini et al., 2020). Secondly, our results showed an increased activation of  
533 the medial extent of the SPL (i.e., precuneus) for the biomimetic surface, with respect to both  
534 control surfaces, in line with functional interactions (e.g., somatomotor function) between the  
535 precuneus and the thalamus (Cunningham et al., 2017; Gamberini et al., 2020). In this light, the  
536 shared connectivity between the precuneus and the extrastriate body area (EBA) (Zeharia et al.,  
537 2019), which showed an enhanced activity in the biomimetic surface condition, is consistent  
538 with the role of the EBA in enhancing the local spatial processing of body information on the

539 direction of a stimuli out of view (Striem-Amit & Amedi, 2014; Urgesi et al., 2007), such as  
540 the skin stretch under the feet in the current study.

541 The shorter latencies of the SEP observed when the participants stood on the translating  
542 biomimetic surface could suggest some contribution of muscle-stretch receptors, as it is well-  
543 established that muscle spindle endings are extremely sensitive stretch receptors (see Starr et  
544 al., 1981; Cohen et al., 1985). However, the evoked potentials that arise from the stimulation  
545 of the lower limbs endings exhibit much shorter latencies (i.e., 20-65 ms; Starr et al., 1981;  
546 Cohen et al., 1985) than those observed in the current study (126 ms, for the biomimetic  
547 surface). Furthermore, the increased activity of the leg muscles induced by the translation of  
548 the biomimetic surface occurred ~160 ms after the onset of the translation, i.e., after the P1  
549 occurrence. This reduces the possibility for a significant role of muscle-stretch receptors in  
550 generating the SEP when the participants stood on the translating surface, irrespectively of the  
551 type of supporting surface. Neither is vestibular input a likely candidate for evoking the cortical  
552 response, as P1 and N1 had shorter latencies than the latency with which the head reached the  
553 acceleration threshold for activating vestibular receptors (i.e., 207 ms, for the biomimetic  
554 surface).

555

#### 556 *Decreased balance task difficulty when standing on the biomimetic surface*

557 Finally, the results of theta oscillations analyses were consistent with the likely role of  
558 the left PPC in attentional processes (Hülsdünker et al., 2015; Mierau et al., 2017). Our  
559 participants showed a significant decreased power of theta oscillations in the left PPC when  
560 they stood on the biomimetic surface compared to the control surfaces (i.e., grooved and  
561 smooth). Since theta oscillations are considered as a neural correlate of a need for attentional  
562 demand in challenging balance tasks (i.e., theta power increases with increased attentional  
563 demand, Sipp et al., 2013; Hülsdünker et al., 2015; Gebel et al., 2020), the significant decrease  
564 of theta-band power with the biomimetic surface may reflect a decrease in the attentional  
565 demand and a down modulation in the difficulty of the task (Vuillerme & Nafati, 2007).  
566 Alternatively, the increased theta power, observed when standing on both control surfaces, may  
567 witness the increase attentional and cognitive demands. This is consistent with the greater  
568 activities observed within the pre-motor cortex (e.g., SMA) and ACC of the left hemisphere  
569 observed when the tactile salience of the surface decreases, as when standing on a smooth  
570 surface (as compared to either the biomimetic or grooved surfaces). Previous studies have  
571 suggested that the SMA plays an important role in the control of demanding balance tasks  
572 (Taubert et al., 2010, 2011). This was notably evidenced by the significant structural and

573 functional adaptation of the SMA activity after balance training (Taubert et al., 2011).  
574 Therefore, the enhanced activity of the SMA, found when individuals stood on the smooth  
575 surface, may suggest that the standing task was more demanding with this surface than with  
576 textured surfaces (biomimetic or grooved). The increased activity observed in the ACC would  
577 also be consistent with this suggestion as the role of this cortical region is well-recognized when  
578 individuals are uncertain about fulfilling the required task appropriately (e.g., Gemba et al.  
579 1986) or in error-recognition (Holroyd et al., 1998; see Holroyd & Coles, 2002, for a review).  
580 These interpretations are also supported by the proposed function of the ACC in the regulation  
581 of attention and cognitive control (Botvinick et al., 2001; Bryden et al., 2011; Petersen &  
582 Posner, 2012). Enhancing the need for attention when standing on a smooth surface could be a  
583 mean for withholding potentially erroneous responses in conditions with impoverished tactile  
584 cues on platform translation until other sensory modalities (e.g., vestibular, visual) can resolve  
585 the ambiguity of the support displacement. In addition to the increased theta oscillations power  
586 for the control grooved surface, the source analyses revealed an increased activation of the right  
587 PPC. These findings are consistent with the crucial role of this cortical area in the processing of  
588 somaesthetic gravitational information for postural control, as shown in neglect patients after  
589 right hemispheric strokes (Pérennou, 2006).

590 Overall, our results point to a reduced difficulty of the balance task when standing on a  
591 biomimetic surface. In *Experiment 2*, we tested the hypothesis that standing on such a surface  
592 benefits postural control when the balance task is challenged by increasing the attentional load  
593 Indeed, because postural control is known to require attention (Lajoie et al., 1993), therefore  
594 the postural perturbation observed when performing a simultaneous cognitive task would be  
595 due to the sharing of limited attentional resources (Stelmach et al., 1990; Chen et al., 1996;  
596 Shumway-Cook & Woollacott, 2000; see Woollacott & Shumway-Cook, 2002 for a review).  
597

## 598 **Experiment 2**

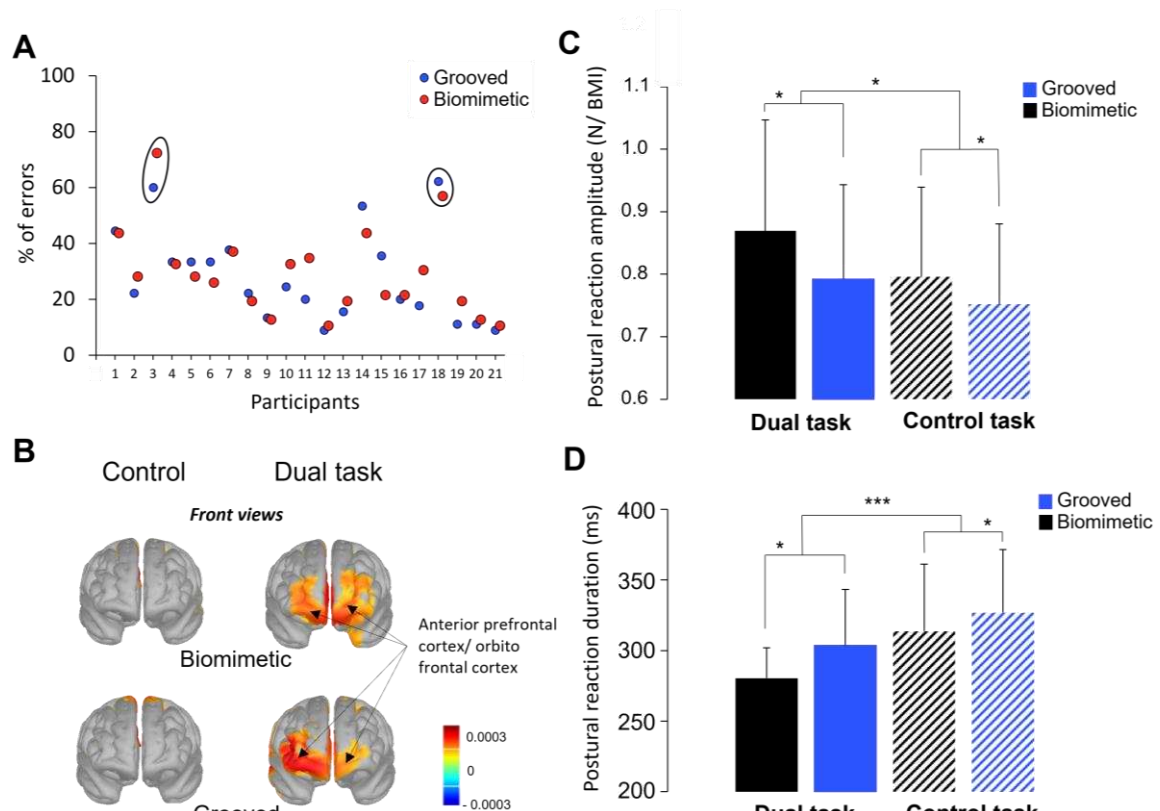
### 599 **Results**

#### 600 *Cognitive task performance*

601 To verify whether the participants' performance in the cognitive task differed when  
602 standing on the moving biomimetic and the grooved surfaces, we analysed the averaged  
603 percentage of errors reporting the number of times that 7 was part of the series of 3-digit  
604 numbers spelled out with high speed. A paired t-test did not reveal significant difference in the  
605 percentage of errors between the biomimetic and the grooved surfaces ( $t_{20} = -0.20$ ;  $p = 0.85$ ; 24

606  $\pm 11.5\%$ ). As shown in Fig. 6A, 2 out 21 participants exhibited values three times above the  
 607 standard deviation of the mean (i.e., 59% and 66% of errors). These large errors suggest that  
 608 the task was too difficult for these participants or that they did not allocate enough attentional  
 609 resources to the cognitive task. These participants were excluded from the analyses.

610 Furthermore, the activity observed over both the anterior prefrontal and orbito-frontal  
 611 cortices during the last part of the counting (i.e., over a 2000 ms interval before the platform  
 612 translation) were greater in the dual task than in the single task (Fig. 6B). This confirmed the  
 613 participants' engagement in the cognitive task (McGuire & Botvinick, 2010; Wallis, 2007).  
 614 Note that no such activities of the frontal lobe were observed in the 2 participants that were  
 615 discarded from the analyses, due to their high error rate.



616  
 617  
 618 **Figure 6.** **A.** Percentage of errors for the cognitive task of each participant on both surfaces  
 619 (grooved, biomimetic). **B.** Source localization during the time window from -2000 to 0 ms  
 620 latency interval on both surfaces (grooved, biomimetic) during solely the motor task (i.e.,  
 621 control) and the dual task. We display the front view of the sources are projected on a cortical  
 622 template (MNI's Colin 27). **C.** Mean postural reaction amplitude normalized by the BMI for all  
 623 participants computed on both surfaces (grooved, biomimetic) during solely the motor task  
 624 (i.e., control) and the dual task. Error bars represent standard deviation across participants; \*  
 625  $p < 0.05$  **D.** Mean postural reaction latency for all participants ( $n = 21$ ) computed on both  
 626 surfaces (grooved, biomimetic) during solely the motor task (i.e., control) and the dual task.  
 627 Error bars represent standard deviation across participants; \*\*\*  $p < 0.001$ .

628 *Postural reaction in response to surface translation*

629 The ANOVA indicated that postural reaction was of greater magnitude when performing  
630 the dual task (combined cognitive and motor tasks) than the single motor task ( $F_{1,18} = 4.78$ ;  
631  $p=0.04$ ), and when standing on the biomimetic as compared to the grooved surface ( $F_{1,18} = 5.92$ ,  
632  $p=0.03$ ) (Fig. 6C). No significant interaction was observed between Task and Surface ( $F_{1,18} =$   
633  $0.76$ ;  $p=0.39$ ). The ANOVA also revealed that the duration of the postural reaction was shorter  
634 when performing a dual task ( $F_{1,18} = 21.183$ ;  $p < 0.05$ ) and when standing on the biomimetic  
635 surface ( $F_{1,18} = 6.95$ ;  $p = 0.02$ ) (Fig. 6D). The interaction Task x Surface was not significant  
636 ( $F_{1,18} = 0.43$ ;  $p=0.51$ ).

637 Although the ANOVAs performed on the variables related to the postural reaction did  
638 not reveal significant Task x Surface interactions, the inspection of the results shown in Fig. 6  
639 suggests that the most efficient postural reaction was found when participants stood on the  
640 biomimetic surface in the dual-task condition (i.e., greater amplitude (Fig. 6C) and smaller  
641 duration (Fig. 6D) of the postural reaction). In support with this assumption, the results of  
642 planned contrasts post-hoc tests revealed that the postural reaction had significantly greater  
643 amplitude ( $F = 10.51$ ;  $p < 0.005$ ) and smaller duration ( $F = 37.70$ ;  $p < 0.001$ ) when standing on  
644 a biomimetic surface, rather than in the 3 other conditions.

645 **Discussion**

646 The intriguing result of *Experiment 2* is that the postural reaction observed during the  
647 platform translation had shorter duration and greater magnitude in the dual task than in the  
648 single task, irrespectively of the standing surfaces. These behavioral features comply with the  
649 spatiotemporal characteristics of an efficient postural reaction (Ikai et al., 2003; Horak et al.,  
650 1997 for a review). They were observed to a greater extent when the participants stood on the  
651 biomimetic surface. Therefore, the participants' engagement in the cognitive task did not have  
652 a deleterious consequence on the postural control as often reported in previous studies (e.g.,  
653 Shumway-Cook et al., 1997; Kerr et al., 1985; Rankin et al., 2000; Melzer et al., 2001). The  
654 greatest efficiency of the postural reaction observed in participants standing on the biomimetic  
655 surface could stem from a greater capacity to shift the attentional focus from the primary motor  
656 task to the secondary cognitive task. Such external focus is known to diminish motor-related  
657 conscious attentional processes (Vuillerme & Nafati, 2007; Wulf & Prinz, 2001, for a review)  
658 compared to an internal focus of attention (Sherwood et al., 2020), and improve motor  
659 performance. This has been clearly demonstrated by Wulf et al. (1998) in a study in which  
660 participants had to make oscillatory movements (ski-type slalom movements) when standing

661 of platform mounted on wheels that ran laterally on two bowed rails. Elastic rubber belts  
662 attached to the platform ensured that the platform returned to the center position during the  
663 oscillatory movements. The authors showed that the motor performance decreased when the  
664 participants' attention was focused on the force that the feet should exert on the supporting  
665 platform (i.e., internal focus) as compared to when their attention was focused on the wheels of  
666 the platform (external focus). These results, combined with those of *Experiment 1* showing  
667 similar postural reactions between the different surfaces, suggest that during small accelerations  
668 of the standing platform, the advantage of standing on a biomimetic surface to safeguard  
669 stability is expressed when one is involved in a dual task (*Experiment 2*). Although it is often  
670 the case that one is engaged in a cognitive task while standing (e.g., listening to people, singing  
671 while showering, etc.), greater platform accelerations could be needed for the biomimetic  
672 surface to improve postural reactions compared to other types of surface.

673 It is possible that the equilibrium demands in response to support translations decreased  
674 when standing on a biomimetic surface, as also suggested by the smaller theta power observed  
675 in *Experiment 1* with this surface. The biomimetic surface may therefore facilitate the use of  
676 low-level sensorimotor loops, which are less permeable to cognitive load and which enable  
677 speedy performance (see Wulf & Prinz, 2001 for a review). As mentioned in Discussion 1,  
678 thalamic projections to the left pre-cuneus (Cunningham et al., 2017; Gamberini et al., 2020),  
679 which has dense interconnections with the motor and premotor cortices (see Krubitzer et  
680 Disbrow 2008 for a review) may have contributed to the facilitation of the neural responses to  
681 the tactile stimulation observed with the biomimetic surface (i.e., increased P1N1 SEP). These  
682 thalamocortical connections areas could constitute the neural underpinning of the efficient  
683 spatiotemporal pattern of the postural reaction when standing on the biomimetic surface.

684

685

686

## 687 **Acknowledgement**

688 We thank Frédéric Pous (Institut des Sciences du Mouvement, Marseille) for his  
689 assistance in the fabrication of the supporting surfaces

690

691

692

693

694

695

696

697

698 **References**

699 Allen, D. P., & MacKinnon, C. D. (2010). Time-frequency analysis of movement-related  
700 spectral power in EEG during repetitive movements : A comparison of methods.  
701 *Journal of Neuroscience Methods*, 186(1), 107-115.  
702 <https://doi.org/10.1016/j.jneumeth.2009.10.022>

703 Altenmüller, E., Berger, W., Prokop, T., Trippel, M., & Dietz, V. (1995). Modulation of sural  
704 nerve somatosensory evoked potentials during stance and different phases of the step-  
705 cycle. *Electroencephalography and Clinical Neurophysiology/Evoked Potentials  
706 Section*, 96(6), 516-525. [https://doi.org/10.1016/0013-4694\(95\)00093-E](https://doi.org/10.1016/0013-4694(95)00093-E)

707 Basdogan, C., Giraud, F., Levesque, V., & Choi, S. (2020). A review of surface haptics:  
708 enabling tactile effects on touch surfaces. *IEEE Transactions on Haptics*, 13(3),  
709 450-470. <https://doi.org/10.1109/TOH.2020.2990712>

710 Benjamini, Y., & Hochberg, Y. (1995). Controlling the false discovery rate: a practical and  
711 powerful approach to multiple testing. *Journal of the Royal Statistical Society: Series  
712 B (Methodological)*, 57(1), 289-300. <https://doi.org/10.1111/j.2517-6161.1995.tb02031.x>

713 Bensmaia, S. J., Denchev, P. V., Dammann, F. J., Craig, J. C., & Hsiao, S. S. (2008). The  
714 representation of stimulus orientation in the early stages of somatosensory processing.  
715 *The Journal of Neuroscience*, 28(3), 776-786.  
716 <https://doi.org/10.1523/JNEUROSCI.4162-07.2008>

717 Boisgontier, M., Mignardot, J.-B., Nougier, V., Olivier, I., & Palluel, E. (2011). Le coût  
718 attentionnel associé aux fonctions exécutives impliquées dans le contrôle postural.  
719 *Science & Motricité*, 74, 53-64. <https://doi.org/10.1051/sm/2011106>

720 Botvinick, M. M., Braver, T. S., Barch, D. M., Carter, C. S., & Cohen, J. D. (2001). Conflict  
721 monitoring and cognitive control. *Psychological Review*, 108(3), 624-652.  
722 <https://doi.org/10.1037/0033-295x.108.3.624>

724 Bryden, D. W., Johnson, E. E., Tobia, S. C., Kashtelyan, V., & Roesch, M. R. (2011).

725 Attention for learning signals in anterior cingulate cortex. *The Journal of*  
726 *Neuroscience*, 31(50), 18266-18274. <https://doi.org/10.1523/JNEUROSCI.4715-11.2011>

727

728 Camillieri, B., Bueno, M.-A., Juan, B., Lemaire-Semail, B., Mouchnino, L., & Fabre, M.

729 (2018). From finger friction and induced vibrations to brain activation : Tactile

730 comparison between real and virtual textile fabrics. *Tribology International*, 126,

731 283-296. <https://doi.org/10.1016/j.triboint.2018.05.031>

732 Carpenter, M. G., Murnaghan, C. D., & Inglis, J. T. (2010). Shifting the balance : Evidence of

733 an exploratory role for postural sway. *Neuroscience*, 171(1), 196-204.

734 <https://doi.org/10.1016/j.neuroscience.2010.08.030>

735 Case, L., Laubacher, C. M., Olausson, H., Wang, B., Spagnolo, P. A., & Bushnell, C. M.

736 (2016). Encoding of touch intensity but not pleasantness in human primary

737 somatosensory cortex. *The Journal of Neuroscience*, 36(21), 5850-5860.

738 <https://doi.org/10.1523/jneurosci.1130-15.2016>

739 Chand, G. B., & Dhamala, M. (2017). Interactions between the anterior cingulate-insula

740 network and the fronto-parietal network during perceptual decision-making.

741 *NeuroImage*, 152, 381-389. <https://doi.org/10.1016/j.neuroimage.2017.03.014>

742 Chen, H.-C., Schultz, A. B., Ashton-Miller, J. A., Giordani, B., Alexander, N. B., & Guire, K.

743 E. (1996). Stepping over obstacles: dividing attention impairs performance of old

744 more than young adults. *The Journals of Gerontology Series A: Biological Sciences*

745 and *Medical Sciences*, 51A(3), M116-M122.

746 <https://doi.org/10.1093/gerona/51A.3.M116>

747 Cohen, L. G., Starr, A., & Pratt, H. (1985). Cerebral somatosensory potentials evoked by  
748 muscle stretch, cutaneous taps and electrical stimulation of peripheral nerves in the  
749 lower limbs in man. *Brain*, 108(1), 103-121. <https://doi.org/10.1093/brain/108.1.103>

750 Cornuault, P.-H., Carpentier, L., Bueno, M.-A., Cote, J.-M., & Monteil, G. (2015). Influence  
751 of physico-chemical, mechanical and morphological fingerpad properties on the  
752 frictional distinction of sticky/slippery surfaces. *Journal of The Royal Society  
753 Interface*, 12(110), 20150495. <https://doi.org/10.1098/rsif.2015.0495>

754 Cummins, H., & Midlo, C. (1926). Palmar and plantar epidermal ridge configurations  
755 (dermatoglyphics) in European-Americans. *American Journal of Physical  
756 Anthropology*, 9(4), 471-502. <https://doi.org/10.1002/ajpa.1330090422>

757 Cunningham, S. I., Tomasi, D., & Volkow, N. D. (2017). Structural and functional  
758 connectivity of the precuneus and thalamus to the default mode network. *Human  
759 Brain Mapping*, 38, 938–956. <https://doi.org/10.1002/hbm.23429>

760 Dale, A. M., Liu, A. K., Fischl, B. R., Buckner, R. L., Belliveau, J. W., Lewine, J. D., &  
761 Halgren, E. (2000). Dynamic statistical parametric mapping: combining fMRI and  
762 meg for high-resolution imaging of cortical activity. *Neuron*, 26(1), 55-67.  
763 [https://doi.org/10.1016/S0896-6273\(00\)81138-1](https://doi.org/10.1016/S0896-6273(00)81138-1)

764 de Lafuente, V., & Romo, R. (2006). Neural correlate of subjective sensory experience  
765 gradually builds up across cortical areas. *Proceedings of the National Academy of  
766 Sciences of the United States of America (PNAS)*.  
767 <https://doi.org/10.1073/pnas.0605826103>

768 Desmedt, J. E., & Robertson, D. (1977). Differential enhancement of early and late  
769 components of the cerebral somatosensory evoked potentials during forced-paced  
770 cognitive tasks in man. *The Journal of Physiology*, 271, 761-782.  
771 <https://doi.org/10.1113/jphysiol.1977.sp012025>

772 Destrieux, C., Fischl, B., Dale, A., & Halgren, E. (2010). Automatic parcellation of human  
773 cortical gyri and sulci using standard anatomical nomenclature. *NeuroImage*, 53(1),  
774 1-15. <https://doi.org/10.1016/j.neuroimage.2010.06.010>

775 Fearing, R. S., & Hollerbach, J. M. (1985). Basic solid mechanics for tactile sensing. *The*  
776 *International Journal of Robotics Research*, 4(3), 40-54.  
777 <https://doi.org/10.1109/ROBOT.1984.1087171>

778 Gamberini, M., Passarelli, L., Impieri, D., Worthy, K. H., Burman, K. J., Fattori, P., Galletti,  
779 C., Rosa, M. G. P., & Bakola, S. (2020). Thalamic afferents emphasize the different  
780 functions of macaque precuneate areas. *Brain Structure & Function*, 225(2), 853-870.  
781 <https://doi.org/10.1007/s00429-020-02045-2>

782 Gebel, A., Lehmann, T., & Granacher, U. (2020). Balance task difficulty affects postural  
783 sway and cortical activity in healthy adolescents. *Experimental Brain Research*,  
784 238(5), 1323-1333. <https://doi.org/10.1007/s00221-020-05810-1>

785 Gemba, H., Sasaki, K., & Brooks, V. B. (1986). « Error » potentials in limbic cortex (anterior  
786 cingulate area 24) of monkeys during motor learning. *Neuroscience Letters*, 70(2),  
787 223-227. [https://doi.org/10.1016/0304-3940\(86\)90467-2](https://doi.org/10.1016/0304-3940(86)90467-2)

788 Gianna, C., Heimbrand, S., & Gresty, M. (1996). Thresholds for detection of motion direction  
789 during passive lateral whole-body acceleration in normal subjects and patients with  
790 bilateral loss of labyrinthine function. *Brain Research Bulletin*, 40(5-6), 443-447.  
791 [https://doi.org/10.1016/0361-9230\(96\)00140-2](https://doi.org/10.1016/0361-9230(96)00140-2)

792 Hämäläinen, H., Kekoni, J., Sams, M., Reinikainen, K., & Näätänen, R. (1990). Human  
793 somatosensory evoked potentials to mechanical pulses and vibration : Contributions of  
794 SI and SII somatosensory cortices to P50 and P100 components.  
795 *Electroencephalography and Clinical Neurophysiology*, 75(1), 13-21.  
796 [https://doi.org/10.1016/0013-4694\(90\)90148-D](https://doi.org/10.1016/0013-4694(90)90148-D)

797 Hollins, M., & Risner, S. R. (2000). Evidence for the duplex theory of tactile texture  
798 perception. *Perception & Psychophysics*, 62(4), 695-705.  
799 <https://doi.org/10.3758/bf03206916>

800 Holroyd, C. B., & Coles, M. G. H. (2002). The neural basis of human error processing :  
801 Reinforcement learning, dopamine, and the error-related negativity. *Psychological  
802 Review*, 109(4), 679-709. <https://doi.org/10.1037/0033-295X.109.4.679>

803 Holroyd, C. B., Dien, J., & Coles, M. G. (1998). Error-related scalp potentials elicited by  
804 hand and foot movements : Evidence for an output-independent error-processing  
805 system in humans. *Neuroscience Letters*, 242(2), 65-68.  
806 [https://doi.org/10.1016/s0304-3940\(98\)00035-4](https://doi.org/10.1016/s0304-3940(98)00035-4)

807 Horak, F. B., Henry, S. M., & Shumway-Cook, A. (1997). Postural perturbations: New  
808 insights for treatment of balance disorders. *Physical Therapy*, 77(5), 517-533.  
809 <https://doi.org/10.1093/ptj/77.5.517>

810 Hülsdünker, T., Mierau, A., Neeb, C., Kleinöder, H., & Strüder, H. K. (2015). Cortical  
811 processes associated with continuous balance control as revealed by EEG spectral  
812 power. *Neuroscience Letters*, 592, 5. <https://doi.org/10.1016/j.neulet.2015.02.049>

813 Ikai, T., Kamikubo, T., Takehara, I., Nishi, M., & Miyano, S. (2003). Dynamic postural  
814 control in patients with hemiparesis. *American Journal of Physical Medicine &  
815 Rehabilitation*, 82(6), 463-469.  
816 <https://doi.org/10.1097/01.PHM.0000069192.32183.A7>

817 Impieri, D., Gamberini, M., Passarelli, L., Rosa, M. G. P., & Galletti, C. (2018). Thalamo-  
818 cortical projections to the macaque superior parietal lobule areas PEc and PE. *Journal  
819 of Comparative Neurology*, 526(6), 1041-1056. <https://doi.org/10.1002/cne.24389>

820 Jacobs, J. V., Fujiwara, K., Tomita, H., Furune, N., Kunita, K., & Horak, F. B. (2008).  
821 Changes in the activity of the cerebral cortex relate to postural response modification

822 when warned of a perturbation. *Clinical Neurophysiology*, 119(6), 1431-1442.

823 <https://doi.org/10.1016/j.clinph.2008.02.015>

824 Jeon, W., Griffin, L., & Hsiao, H.-Y. (2021). Effects of initial foot position on postural  
825 responses to lateral standing surface perturbations in younger and older adults. *Gait &*  
826 *Posture*, 90, 449-456. <https://doi.org/10.1016/j.gaitpost.2021.09.193>

827 Johansson, R. S., & Vallbo, Å. B. (1983). Tactile sensory coding in the glabrous skin of the  
828 human hand. *Trends in Neurosciences*, 6, 27-32. [https://doi.org/10.1016/0166-2236\(83\)90011-5](https://doi.org/10.1016/0166-2236(83)90011-5)

829 Kennedy, P. M., & Inglis, J. T. (2002). Distribution and behaviour of glabrous cutaneous  
830 receptors in the human foot sole. *The Journal of Physiology*, 538(3), 995-1002.  
831 <https://doi.org/10.1113/jphysiol.2001.013087>

832 Kerr, B., Condon, S., & McDonald, L. (1985). Cognitive spatial processing and the regulation  
833 of posture. *Journal of Experimental Psychology; Human Perception and*  
834 *Performance*, Vol. 11(No. 5), 617-622. <https://doi.org/10.1037//0096-1523.11.5.617>

835 Klein, P., Sommerfeld, P., & Meddeb, G. (2008). *Biomécanique des membres inférieures*  
836 (Elsevier Masson).  
837

838 Krubitzer, L., & Disbrow, E. (2008). *The Evolution of Parietal Areas Involved in Hand Use in*  
839 *Primates. The Senses: A Comprehensive Reference*, Vol. 6, Chapter 10, 183-214.  
840 <https://doi.org/10.1016/B978-012370880-9.00352-2>

841 Lajoie, Y., Teasdale, N., Bard, C., & Fleury, M. (1993). Attentional demands for static and  
842 dynamic equilibrium. *Experimental Brain Research*, 97(1).  
843 <https://doi.org/10.1007/BF00228824>

844 Latash, M. L., Ferreira, S. S., Wieczorek, S. A., & Duarte, M. (2003). Movement sway:  
845 Changes in postural sway during voluntary shifts of the center of pressure.

846      *Experimental Brain Research*, 150(3), 314-324. <https://doi.org/10.1007/s00221-003-1419-3>

847

848      Lederman, S. J., & Klatzky, R. L. (2009). Haptic perception: A tutorial. *Attention, Perception*  
849      & *Psychophysics*, 71(7), 1439-1459. <https://doi.org/10.3758/APP.71.7.1439>

850      Lhomond, O., Juan, B., Fornerone, T., Cossin, M., Paleressompoule, D., Prince, F., &

851      Mouchnino, L. (2021). Learned overweight internal model can be activated to

852      maintain equilibrium when tactile cues are uncertain: Evidence from cortical and

853      behavioral approaches. *Frontiers in Human Neuroscience*.

854      <https://doi.org/10.3389/FNHUM.2021.635611>

855      Lhomond, O., Teasdale, N., Simoneau, M., & Mouchnino, L. (2016). Neural consequences of

856      increasing body weight: Evidence from somatosensory evoked potentials and the

857      frequency-specificity of brain oscillations. *Frontiers in Human Neuroscience*, 10.

858      <https://doi.org/10.3389/fnhum.2016.00318>

859      Lin, Y.-Y., Shih, Y.-H., Chen, J.-T., Hsieh, J.-C., Yeh, T.-C., Liao, K.-K., Kao, C.-D., Lin,

860      K.-P., Wu, Z.-A., & Ho, L.-T. (2003). Differential effects of stimulus intensity on

861      peripheral and neuromagnetic cortical responses to median nerve stimulation.

862      *NeuroImage*, 20(2), 909-917. [https://doi.org/10.1016/S1053-8119\(03\)00387-2](https://doi.org/10.1016/S1053-8119(03)00387-2)

863      Maki, B. E., & McIlroy, W. E. (2007). Cognitive demands and cortical control of human

864      balance-recovery reactions. *Journal of Neural Transmission*, 114(10), 1279-1296.

865      <https://doi.org/10.1007/s00702-007-0764-y>

866      Massimiani, V., Benjamin, W., Eric, C., Pierre-Henri, C., Jenny, F., & Francesco, M. (2020).

867      The role of mechanical stimuli on hedonistic and topographical discrimination of

868      textures. *Tribology International*, 143, 9.

869      <https://doi.org/10.1016/j.triboint.2019.106082>

870 Mauguier, F., Merlet, I., Forss, N., Vanni, S., Jousmäki, V., Adeleine, P., & Hari, R. (1997).

871 Activation of a distributed somatosensory cortical network in the human brain : A  
872 dipole modelling study of magnetic fields evoked by median nerve stimulation. Part  
873 II: effects of stimulus rate, attention and stimulus detection. *Electroencephalography*  
874 and *Clinical Neurophysiology/Evoked Potentials Section*, 104(4), 290-295.  
875 [https://doi.org/10.1016/S0013-4694\(97\)00018-7](https://doi.org/10.1016/S0013-4694(97)00018-7)

876 McGuire, J. T., & Botvinick, M. M. (2010). Prefrontal cortex, cognitive control, and the  
877 registration of decision costs. *Proceedings of the National Academy of Sciences of the  
878 United States of America*, 107(17), 7922-7926.  
879 <https://doi.org/10.1073/pnas.0910662107>

880 Melzer, I., Benjuya, N., & Kaplanski, J. (2001). Age-related changes of postural control:  
881 Effect of cognitive tasks. *Gerontology*, 47(4), 189-194.  
882 <https://doi.org/10.1159/000052797>

883 Mierau, A., Pester, B., Hülsdünker, T., Schiecke, K., Strüder, H. K., & Witte, H. (2017).  
884 Cortical correlates of human balance control. *Brain Topogr*, 434-446.  
885 <https://doi.org/10.1007/s10548-017-0567-x>

886 Mochizuki, L., Duarte, M., Amadio, A. C., Zatsiorsky, V. M., & Latash, M. L. (2006).  
887 Changes in postural sway and its fractions in conditions of postural instability. *Journal  
888 of Applied Biomechanics*, 22(1), 51-60. <https://doi.org/10.1123/jab.22.1.51>

889 Morasso, P. G., & Schieppati, M. (1999). Can muscle stiffness alone stabilize upright  
890 standing? *Journal of Neurophysiology*, 82(3), 1622-1626.  
891 <https://doi.org/10.1152/jn.1999.82.3.1622>

892 Mouchnino, L., & Blouin, J. (2013). When standing on a moving support, cutaneous inputs  
893 provide sufficient information to plan the anticipatory postural adjustments for gait  
894 initiation. *PLoS ONE*, 8(2), e55081. <https://doi.org/10.1371/journal.pone.0055081>

895 Murnaghan, C. D., Horslen, B. C., Inglis, J. T., & Carpenter, M. G. (2011). Exploratory  
896 behavior during stance persists with visual feedback. *Neuroscience*, 195, 54-59.  
897 <https://doi.org/10.1016/j.neuroscience.2011.08.020>

898 Padberg, J., Cerkevich, C., Engle, J., Rajan, A. T., Recanzone, G., Kaas, J., & Krubitzer, L.  
899 (2009). Thalamocortical connections of parietal somatosensory cortical fields in  
900 macaque monkeys are highly divergent and convergent. *Cerebral Cortex*, 19(9),  
901 2038-2064. <https://doi.org/10.1093/cercor/bhn229>

902 Pearson, R. C. A., Brodal, P., & Powell, T. P. S. (1978). The projection of the thalamus upon  
903 the parietal lobe in the monkey. *Brain Research*, 143-148.  
904 [https://doi.org/10.1016/0006-8993\(78\)90440-7](https://doi.org/10.1016/0006-8993(78)90440-7)

905 Pérennou, D. (2006). Postural disorders and spatial neglect in stroke patients: A strong  
906 association. *Restorative Neurology and Neuroscience*, 24(4-6), 319-334.

907 Petersen, S. E., & Posner, M. I. (2012). The attention system of the human brain: 20 years  
908 after. *Annual Review of Neuroscience*, 35, 73-89. <https://doi.org/10.1146/annurev-neuro-062111-150525>

910 Peyre, K., Tourlonias, M., Bueno, M.-A., & Rossi, R. (2017). Conception d'un doigt artificiel  
911 à fibre optique polymérique pour application du toucher de surface textile.

912 Pietrosimone, B. G., & Gribble, P. A. (2012). Chronic ankle instability and corticomotor  
913 excitability of the fibularis longus muscle. *Journal of Athletic Training*, 47(6),  
914 621-626. <https://doi.org/10.4085/1062-6050-47.6.11>

915 Ponz, A., Montant, M., Liegeois-Chauvel, C., Silva, C., Braun, M., Jacobs, A. M., & Ziegler,  
916 J. C. (2014). Emotion processing in words: A test of the neural re-use hypothesis using  
917 surface and intracranial EEG. *Social Cognitive and Affective Neuroscience*, 9(5),  
918 619-627. <https://doi.org/10.1093/scan/nst034>

919 Prevost, A., Scheibert, J., & Debrégeas, G. (2009). Effect of fingerprints orientation on skin  
920 vibrations during tactile exploration of textured surfaces. *Communicative &*  
921 *Integrative Biology*, 2(5), 422-424. <https://doi.org/10.4161/cib.2.5.9052>

922 Rabinowicz, E. (1956). When two substances rub against each other, they frequently stick and  
923 then slip. The phenomenon accounts for the squeak of bearings, the music of violins  
924 and many other sounds of our daily experience. *SCIENTIFIC AMERICAN*, 11.

925 Rankin, J. K., Woollacott, M. H., Shumway-Cook, A., & Brown, L. A. (2000). Cognitive  
926 influence on postural stability: A neuromuscular analysis in young and older adults.  
927 *The Journals of Gerontology Series A: Biological Sciences and Medical Sciences*,  
928 55(3), M112-M119. <https://doi.org/10.1093/gerona/55.3.M112>

929 Redfern, M. S., Muller, M. L. T. M., Jennings, J. R., & Furman, J. M. (2002). Attentional  
930 dynamics in postural control during perturbations in young and older adults. *The*  
931 *Journals of Gerontology Series A: Biological Sciences and Medical Sciences*, 57(8),  
932 B298-B303. <https://doi.org/10.1093/gerona/57.8.B298>

933 Riley, M., Mitra, S., Stoffregen, T., & Turvey, M. (1997). Influences of body lean and vision  
934 on unperturbed postural sway. *Motor Control*, 1, 229-246.  
935 <https://doi.org/10.1123/mcj.1.3.229>

936 Romo, R., & de Lafuente, V. (2012). Conversion of sensory signals into perceptual decisions.  
937 *Progress in Neurobiology*, 35. <https://doi.org/10.1016/j.pneurobio.2012.03.007>

938 Salinas, E., Hernández, A., Zainos, A., & Romo, R. (2000). Periodicity and firing rate as  
939 candidate neural codes for the frequency of vibrotactile stimuli. *The Journal of*  
940 *Neuroscience*, 20(14), 5503-5515. <https://doi.org/10.1523/JNEUROSCI.20-14-05503.2000>

942 Saradjian, A. H., Teasdale, N., Blouin, J., & Mouchnino, L. (2019). Independent early and  
943 late sensory processes for proprioceptive integration when planning a step. *Cerebral  
944 Cortex*, 29(6), 2353-2365. <https://doi.org/10.1093/cercor/bhy104>

945 Sarma, H. (2020). A comparative study of the toe print and fingerprint distribution in indo  
946 Mongolian race.

947 Sherwood, D. E., Lohse, K. R., & Healy, A. F. (2020). The effect of an external and internal  
948 focus of attention on dual-task performance. *Journal of Experimental Psychology:  
949 Human Perception and Performance*, 46(1), 91-104.  
950 <https://doi.org/10.1037/xhp0000698>

951 Shumway-Cook, A., & Woollacott, M. (2000). Attentional demands and postural control: The  
952 effect of sensory context. *The Journals of Gerontology. Series A, Biological Sciences  
953 and Medical Sciences*, 55(1), M10-16. <https://doi.org/10.1093/gerona/55.1.m10>

954 Shumway-Cook, A., Woollacott, M., Kerns, K. A., & Baldwin, M. (1997). The effects of two  
955 types of cognitive tasks on postural stability in older adults with and without a history  
956 of falls. *The Journals of Gerontology Series A: Biological Sciences and Medical  
957 Sciences*, 52A(4), M232-M240. <https://doi.org/10.1093/gerona/52A.4.M232>

958 Sipp, A. R., Gwin, J. T., Makeig, S., & Ferris, D. P. (2013). Loss of balance during balance  
959 beam walking elicits a multifocal theta band electrocortical response. *Journal of  
960 Neurophysiology*, 110(9), 2050-2060. <https://doi.org/10.1152/jn.00744.2012>

961 Sohrabpour, A., Yunfeng, L., & Bin, H. (2015). Estimating underlying neuronal activity from  
962 EEG using an iterative sparse technique. *IEEE Engineering in Medicine and Biology  
963 Society. Annual International Conference, 2015*, 634-637.  
964 <https://doi.org/10.1109/EMBC.2015.7318442>

965 Solis-Escalante, T., Van der Cruis, J., De Kam, D., Van Kordelaar, J., Weerdesteyn, V., &  
966 Schouten, A. C. (2019). Cortical dynamics during preparation and execution of

967 reactive balance responses with distinct postural demands. *NeuroImage*, 188, 557-571.

968 <https://doi.org/10.1016/j.neuroimage.2018.12.045>

969 Starr, A., McKeon, B., Use, N. S., & Burke, D. (1981). Cerebral potentials evoked by muscle

970 stretch in man. *Brain*, 104(1), 149-166. <https://doi.org/10.1093/brain/104.1.149>

971 Stelmach, G. E., Zelaznik, H. N., & Lowe, D. (1990). The influence of aging and attentional

972 demands on recovery from postural instability. *Aging (Milan, Italy)*, 2(2), 155-161.

973 <https://doi.org/10.1007/BF03323910>

974 Striem-Amit, E., & Amedi, A. (2014). Visual cortex extrastriate body-selective area

975 activation in congenitally blind people “seeing” by using sounds. *Current Biology*,

976 24(6), 687-692. <https://doi.org/10.1016/j.cub.2014.02.010>

977 Tang, W., Liu, R., Shi, Y., Hu, C., Bai, S., & Zhu, H. (2020). From finger friction to brain

978 activation: Tactile perception of the roughness of gratings. *Journal of Advanced*

979 *Research*, 21, 129-139. <https://doi.org/10.1016/j.jare.2019.11.001>

980 Taubert, M., Draganski, B., Anwander, A., Müller, K., Horstmann, A., Villringer, A., &

981 Ragert, P. (2010). Dynamic properties of human brain structure: Learning-related

982 changes in cortical areas and associated fiber connections. *The Journal of*

983 *Neuroscience*, 30(35), 11670-11677. <https://doi.org/10.1523/JNEUROSCI.2567-10.2010>

985 Taubert, M., Lohmann, G., Margulies, D. S., Villringer, A., & Ragert, P. (2011). Long-term

986 effects of motor training on resting-state networks and underlying brain structure.

987 *NeuroImage*, 57(4), 1492-1498. <https://doi.org/10.1016/j.neuroimage.2011.05.078>

988 Urgesi, C., Candidi, M., Ionta, S., & Aglioti, S. M. (2007). Representation of body identity

989 and body actions in extrastriate body area and ventral premotor cortex. *Nature*

990 *Neuroscience*, 10(1), 30-31. <https://doi.org/10.1038/nn1815>

991 Valbo, A. B., Olausson, H., Wessberg, J., & Kakuda, N. (1995). Receptive field  
992 characteristics of tactile units with myelinated afferents in hairy skin of human  
993 subjects. *The Journal of Physiology*, 483(Pt 3), 783-795.  
994 <https://doi.org/10.1113/jphysiol.1995.sp020622>

995 Vuillerme, N., & Nafati, G. (2007). How attentional focus on body sway affects postural  
996 control during quiet standing. *Psychological Research*, 71(2), 192-200.  
997 <https://doi.org/10.1007/s00426-005-0018-2>

998 Wallis, J. D. (2007). Orbitofrontal cortex and its contribution to decision-making. *Annual  
999 Review of Neuroscience*, 30, 31-56.  
1000 <https://doi.org/10.1146/annurev.neuro.30.051606.094334>

1001 Weber, A. I., Saal, H. P., Lieber, J. D., Cheng, J.-W., Manfredi, L. R., Iii, J. F. D., &  
1002 Bensmaia, S. J. (2013). Spatial and temporal codes mediate the tactile perception of  
1003 natural textures. *Proceedings of the National Academy of Sciences of the United States  
1004 of America*, 110(42), 17107-17112. <https://doi.org/10.1073/pnas.1305509110>

1005 Woollacott, M., & Shumway-Cook, A. (2002). Attention and the control of posture and gait :  
1006 A review of an emerging area of research. *Gait & Posture*, 16(1), 1-14.  
1007 [https://doi.org/10.1016/S0966-6362\(01\)00156-4](https://doi.org/10.1016/S0966-6362(01)00156-4)

1008 Wulf, G., Höß, M., & Prinz, W. (1998). Instructions for motor learning: Differential effects of  
1009 internal versus external focus of attention. *Journal of Motor Behavior*, 30(2), 169-179.  
1010 <https://doi.org/10.1080/00222899809601334>

1011 Wulf, G., & Prinz, W. (2001). Directing attention to movement effects enhances learning: A  
1012 review. *Psychonomic Bulletin & Review*, 8(4), 648-660.  
1013 <https://doi.org/10.3758/BF03196201>

1014 Zeharia, N., Hofstetter, S., Flash, T., & Amedi, A. (2019). A whole-body sensory-motor  
1015 gradient is revealed in the medial wall of the parietal lobe. *The Journal of*  
1016 *Neuroscience*, 39(40), 7882-7892. <https://doi.org/10.1523/JNEUROSCI.0727-18.2019>  
1017